PHYSICAL REVIEW C **69**, 051304(R) (2004)

$^{16}O+^{16}O$ molecular nature of the superdeformed band of ^{32}S and the evolution of the molecular structure

Masaaki Kimura
RI-beam Science Laboratory, RIKEN (The Institute of Physical and Chemical Research), Wako, Saitama 351-0198, Japan

Hisashi Horiuchi
Department of Physics, Kyoto University, Kitashirakawa, Kyoto 606-8502, Japan
(Received 15 January 2004; published 28 May 2004)

The relation between the superdeformed band of ^{32}S and $^{16}O+^{16}O$ molecular bands is studied by the deformed-basis antisymmetrized molecular dynamics with the Gogny D1S force. It is found that the obtained superdeformed band members of S have a considerable amount of the $^{16}O+^{16}O$ component. Above the superdeformed band, we have obtained two excited rotational bands which have more prominent character of the $^{16}O+^{16}O$ molecular band. These three rotational bands are regarded as a series of $^{16}O+^{16}O$ molecular bands which were predicted by using the unique ^{16}O-^{16}O optical potential. As the excitation energy and principal quantum number of the relative motion increase, the $^{16}O+^{16}O$ cluster structure becomes more prominent but at the same time, the band members are fragmented into several states.

DOI: 10.1103/PhysRevC.69.051304 PACS number(s): 21.10.Re, 21.60.Cs, 27.30.+t

The properties of the $^{16}O+^{16}O$ molecular bands have been studied by many authors with the microscopic cluster models for many years [1–3]. Despite these studies, the microscopic models have not been able to give a conclusive answer. One of the reasons is the fact that the number of the molecular bands, the excitation energies of the band heads, and the moments of the inertia strongly depend on the effective nuclear force. Recently, a rather conclusive answer was given by the studies with the macroscopic model [4,5]. In those studies, the authors used the unique optical potential for the ^{16}O-^{16}O system [6] which was determined without ambiguities from the rainbow scattering in the 1990s after the first discovery of the nuclear rainbow in 1989 [7]. These studies gave the following answers for the lowest three rotational bands whose principal quantum numbers $N=2n+L$ of the relative motion between clusters are $N=24$, 26, and 28, respectively: The lowest Pauli-allowed rotational band ($N=24$) starts from the 0^+ state located at about 9 MeV in the excitation energy (about 8 MeV below the $^{16}O+^{16}O$ threshold), and the energy gap between the $N=24$ and $N=26$ bands and that between, $N=26$ the and $N=28$ bands are both approximately 10 MeV. In Ref. [5], it was proposed that the observed $^{16}O+^{16}O$ molecular states correspond to the third band whose principal quantum number is $N=28$.

Besides the cluster models, the superdeformed structure of ^{32}S has been studied by many authors with the mean-field theories [8–13]. It is largely because the superdeformed structure of ^{32}S is regarded as a key to understand the relation between the superdeformed state and the molecular structure. Indeed, by the Hartree-Fock (HF) and Hartree-Fock-Bogoliubov (HFB) calculations [8–13], it is shown that the superdeformed minimum of the energy surface is well established in each angular momentum, and at the superdeformed local minimum, the wave function shows the two-center-like character. It is also notable that many of the mean-field calculations predict that the superdeformed band starts from the 0^+ located at around 10 MeV which agrees with the bandhead energy of the $N=24$ band obtained from the unique optical potential. Therefore it is conceivable enough that the superdeformed band obtained by the mean-field calculations and the lowest Pauli-allowed $^{16}O+^{16}O$ molecular band ($N=24$) are identical.

In the present study, we aim at clarifying the relation between the superdeformed state and the $^{16}O+^{16}O$ molecular structure. The objectives of this rapid communication are the following two points. (i) To what extent are the superdeformed state and the $^{16}O+^{16}O$ molecular structure related? In the unique optical potential analysis, the factors which distort the $^{16}O+^{16}O$ cluster structure such as the effects of the spin-orbit force and the formation of the deformed mean field are not treated directly. Instead, these factors are renormalized into the optical potential through the extrapolation to the low-energy region. When one treats these factors directly by the microscopic models, the pure $^{16}O+^{16}O$ cluster structure will be distorted and will have a deformed mean-field structure. In other words, the superdeformed states in the mean-field models and the states of the lowest Pauli-allowed $^{16}O+^{16}O$ band of the unique optical potential will be the states which have both characters of the deformed one-body field structure and two cluster structure. (ii) Do the excited states exist in which the excitation energy is spent to excite the relative motion between the clusters? Do they correspond to the $N=26$, and 28 bands obtained from the unique optical potential? When we believe that the superdeformed states of ^{32}S have the considerable amount of $^{16}O+^{16}O$ components, we can expect the excitation mode in which the excitation energy is used to excite the relative motion between the clusters. These excited bands and the superdeformed band can be regarded as a series of the $^{16}O+^{16}O$ molecular band which have the principal quantum number of the relative motion $N=24$, 26 and 28, respectively.

The deformed-basis antisymmetrized molecular dynamics (deformed-basis AMD) [14] combined with the generator coordinate method (GCM [15]) has been used with the Gogny D1S force [16]. For the sake of the completeness, we briefly explain this framework. For more details, the reader is di-

rected to Refs. [14,17]. The intrinsic basis wave function of the system Φ_{int} is expressed by a Slater determinant of single-particle wave packets φ_i. Each single-particle wave packet is composed of spatial part ϕ_i, spin part χ_i, and isospin part τ_i. The spatial part has the form of the deformed Gaussian centered at $\mathbf{Z}_i$,

$$\Phi_{int} = \frac{1}{\sqrt{A!}}\det\{\varphi_i(\mathbf{r}_j)\}, \tag{1}$$

$$\varphi_i(\mathbf{r}_j) = \phi_i(\mathbf{r}_j)\chi_i\tau_i, \tag{2}$$

$$\phi_i(\mathbf{r}) = \exp\{-\nu_x(x - Z_{ix})^2 - \nu_y(y - Z_{iy})^2 - \nu_z(z - Z_{iz})^2\}, \tag{3}$$

$$\chi_i = \alpha_i\chi_\uparrow + \beta_i\chi_\downarrow, \quad \tau_i = \text{proton or neutron}. \tag{4}$$

Here, the centroids of the Gaussian $\mathbf{Z}_i$ and the spin direction α_i and β_i are complex parameters and are dependent on each particle. The width parameters ν_x, ν_y, and ν_z are common to all particles. These variational parameters [$\mathbf{Z}_i$, α_i, β_i and (ν_x, ν_y, ν_z)] are determined by the variational calculation. The variational calculation is made after the parity projection by using parity-projected wave function $\Phi^\pi=[(1\pm P_x)/2]\Phi_{int}$ as the variational wave function. In this study, the variational calculation is made under the constraint of the nuclear deformation parameter β. The advantage of the deformed Gaussian basis as the single-particle wave packet is that it is possible to describe both the deformed one-body-field structure and the cluster structure as well as their mixed structure within the same framework. We can confirm this feature when we consider the two limits of the nuclear structure described by this wave function, the deformed-harmonic-oscillator limit and the cluster limit. The deformed-harmonic-oscillator limit is reached when the centroids of all single-particle wave packets (Re $\mathbf{Z}_i$) are at the center of the nucleus and the single-particle wave packets are deformed. On the contrary, the cluster limit is obtained when the centroids of the single-particle wave packets are separated into the centers of the constituent clusters and the single-particle wave packets are spherical. However, the usage of the deformed Gaussian makes it impossible to separate the wave function of the center-of-mass motion from the internal one. In this study, we approximate its effect to the energy by subtracting the center-of-mass kinetic energy from the total energy.

After the constrained variational calculation for Φ^π, we superimposed the optimized wave functions employing the nuclear deformation parameter β as the generator coordinate (GCM calculation):

$$\Phi^{J^\pi} = cP^J_{MK}\Phi^\pi(\beta_0) + c'P^J_{MK'}\Phi^\pi(\beta_0') + \cdots, \tag{5}$$

where $\Phi^\pi(\beta_0)$ is the optimized wave function under the constraint of the nuclear deformation parameter $\beta=\beta_0$ and P^J_{MK} is the angular momentum projector. The coefficients $c, c', \ldots$ are determined by the diagonalization of the Hamiltonian. The generator coordinates β_0, $\beta_0', \ldots$ are taken from $\beta_0=0$ to $\beta_0\sim 1.05$. This upper limit of β corresponds to the Coulomb barrier and it slightly depends on the angular momentum. The convergence of the GCM solution is confirmed by changing the number of the basis wave functions. For example, in the case of the 0^+ state, 28 basis wave functions are employed.

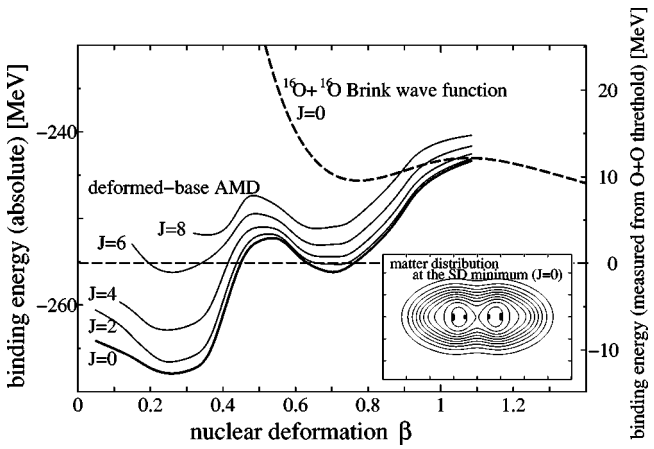

FIG. 1. The energy surface as a function of the nuclear deformation β. The dashed line is for the $J=0$ state obtained by the ^{16}O+^{16}O Brink wave function. Solid lines are for $J=0$, 2, 4, 6, and 8 states obtained by the deformed-basis AMD. The matter density distribution of the deformed-basis AMD wave function at the superdeformed minimum ($J=0$) is also shown. Small black circles in the density distribution represent the centroids of the single-particle wave packets Re $\mathbf{Z}_i$.

To investigate the ^{16}O+^{16}O character of the obtained wave function $\Phi^{J\pi}$, we evaluated the amount of the ^{16}O+^{16}O component in each state. We decompose $\Phi^{J\pi}$ into the ^{16}O+^{16}O component $\Phi_{^{16}O+^{16}O}$ and the residual part $\Phi_r^{J^\pi}$,

$$\Phi^{J\pi} = \alpha\Phi_{^{16}O+^{16}O} + \sqrt{1-\alpha^2}\Phi_r, \langle\Phi^{J^\pi}_{^{16}O+^{16}O}|\Phi_r^{J^\pi}\rangle = 0, \tag{6}$$

and the amount of the ^{16}O+^{16}O component is given as $w^J \equiv |\alpha|^2$. The ^{16}O+^{16}O component is formally represented by the resonating group method (RGM) wave function,

$$\Phi^{J^\pi}_{^{16}O+^{16}O} = \mathcal{A}\{\chi_J(r)Y_{J0}(\hat{r})\phi(^{16}\mathrm{O})\phi(^{16}\mathrm{O})\}, \tag{7}$$

where $\mathcal{A}$ is the antisymmetrizer, $\mathbf{r}$ is the relative coordinate between two ^{16}O clusters and $\phi(^{16}\mathrm{O})$ is the internal wave function of the ^{16}O cluster. $\chi_J(r)$ which is the radial wave function of the relative motion between clusters is so normalized that $\mathcal{A}\{\chi_J(r)\mathrm{Y}_{J0}(\hat{r})\phi(^{16}\mathrm{O})\phi(^{16}\mathrm{O})\}$ is normalized to unity. By using the projection method which is introduced in Refs. [14,18], we project out $\Phi_{^{16}O+^{16}O}$ from Φ^{J^π} and evaluate w_J and $\chi_J(r)$. From $\chi_J(r)$, we also calculate the principal quantum number $N=2n+L$ of each state, where n denotes the number of nodes of $\chi_J(r)$ and $L=J$.

First, we discuss the result of the calculation in which we assume the pure ^{16}O+^{16}O structure of ^{32}S to compare it with that obtained by deformed-basis AMD+GCM. The Brink [19] wave function is used as the ^{16}O+^{16}O wave function. Therefore this result is equivalent to the microscopic cluster model calculation of ^{16}O+^{16}O RGM and ^{16}O+^{16}O GCM. In Fig. 1, the energy surface for the $J=0$ state as a function of

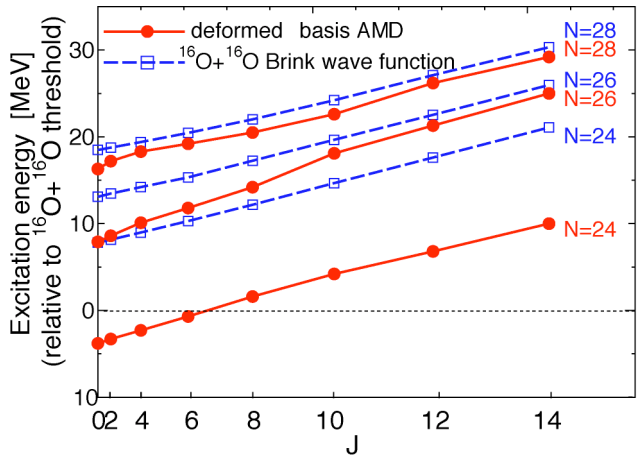

FIG. 2. (Color online) The excitation energies of the $N=24$, 26, and 28 band members obtained by the ^{16}O+^{16}O Brink wave function (dashed lines) and the deformed-basis AMD+GCM (solid lines). The $N=26$ and $N=28$ band members are fragmented into several states in the deformed-basis AMD+GCM calculation and the averaged energies E_{AV} are shown for these bands.

the nuclear deformation is shown (dashed line). We note that the ^{16}O+^{16}O configuration describes more than $4\hbar\omega$ excited states relative to the ground state of ^{32}S, and therefore the ground state and the normal deformed states are not included in this energy surface. It has a energy minimum at $\beta=0.73$ (intercluster distance is 5.0 fm) which corresponds to two touching ^{16}O. The minimum energy is about 8 MeV higher than the ^{16}O+^{16}O threshold energy. After the GCM calculation along this energy surface, we have obtained three rotational bands which have the principal quantum numbers of the relative motion $N=24$, 26, and 28, respectively (dashed lines in Fig. 2). However, their energies are too high to coincide with the rotational bands obtained from the unique optical potential and also with the superdeformed band obtained from the HF and HFB calculations. The energy gaps between these bands (4 MeV between $N=24$ and $N=26$, and 6 MeV between $N=26$ and $N=28$ in the case of 0^+ states) are much smaller than the results of the unique optical potential. We think that these deviations come from the fact that the effects which distort the cluster structure are neglected in this result. We will see below that in fact the effects of the distortion are fairly large.

Next, we present the results of the deformed-basis AMD+GCM calculation. In Fig. 1, the energy surfaces obtained by the deformed-basis AMD are also shown up to 8^+ state (solid lines). Because the deformed-basis AMD wave function does not assume any cluster configuration, the normal deformed states also appear in these energy surfaces. Since we constrain the quadrupole deformation parameter β but not γ in the variational calculation, the values of γ are optimized in each value of β. Around the normal deformed region ($\beta\sim0.3$), we obtained two optimum values of γ. The prolate one ($\gamma=0$) mainly contributes to the ground band after the GCM calculation, while the triaxial one ($\gamma=6°-30°$, the optimum value of γ depends on the angular momentum) contributes to the first excited band. Their excitation energies and the intraband $E2$ transition probabilities

TABLE I. Observed [denoted by (E)] and calculated [denoted by (T)] values of the excitation energies E_x [MeV] and the intraband $B(E2;J\rightarrow J-2)$ $[e^2\ \mathrm{fm}]^4$ of the ground band and the first excited band.

	Ground (T)		Ground (E)		Band I (T)		Band I (E)	
J	E_x	$B(E2)$	E_x	$B(E2)$	E_x	$B(E2)$	E_x	$B(E2)$
0					3.9		3.778	
2	2.3	66	2.23	60 ± 6	4.8	31	4.282	
4	5.75	109	4.459	72 ± 12	10.1	88	6.852	$35.4^{+18.6}_{-8.4}$
6	10.2	130	8.346	>22.2	12.9	98	9.783	

(Table I) show reasonable agreement with experiments and are consistent with the results of the HFB+GCM calculation with the Gogny D1S force [10], though the total binding energy of the ground state underestimates the experimental data by about 2.0 MeV.

Then we discuss the superdeformed states. In each angular momentum state, the superdeformed minimum is well developed and the excitation energy relative to the normal deformed state is around 10 MeV. The energy difference between the deformed-basis AMD and the ^{16}O+^{16}O Brink wave function at the superdeformed minimum is about 10 MeV, which indicates a fairly large effect of the distortion on the excitation energy. Indeed, the deformed-basis AMD wave function deviates from the pure ^{16}O+^{16}O structure. At the superdeformed minimum, the single-particle wave packets are prolate deformed ($\nu_x=\nu_y=0.160\ \mathrm{fm}^{-2}$ and $\nu_z=0.115\ \mathrm{fm}^{-2}$), and the distance between the centroids of the single-particle wave packets are rather small (3.1 fm), though they are still separated into two parts exhibiting a two-center nature. The energy gain due to the distortion of the ^{16}O+^{16}O structure mainly comes from the two-body spin-orbit force and the density dependent force. In the case of the deformed-basis AMD, the expectation value of the two-body spin-orbit force is about −4.5 MeV which must be zero in the ^{16}O+^{16}O wave function. The expectation value of the repulsive density dependent force is about 6 MeV smaller in the deformed-basis AMD and it also indicates the nonsmall deviation from the ^{16}O+^{16}O structure. Though the kinetic energy does not much contribute to lower the energy, its nature is also different. At the superdeformed minimum, the single-particle wave packets are prolately deformed and since the kinetic energy almost linearly depends on the width parameter ν, the kinetic energy in the z direction is eased. However, we found that the deformed-basis AMD wave function at the superdeformed minimum still has a considerable amount of the ^{16}O+^{16}O component ($w^{J=0}=0.57$ for the case of the 0^+ state).

By superposing the deformed-basis AMD wave functions along the energy surface (deformed-basis AMD+GCM), we have obtained three rotational bands above the ground and the first excited bands. The lowest band (superdeformed band), the second lowest band and the third band have large ^{16}O+^{16}O components which have the principal quantum number $N=24$, 26, and 28, respectively. Therefore we consider that these three bands correspond to the $N=24$, 26, and 28 bands of the unique optical potential. We refer to these

bands simply as $N=24$, 26, and 28 bands. The band members of the $N=26$ and 28 bands are fragmented into several states. Namely, there are several states which have the $^{16}O+^{16}O$ component of the same principal quantum number N. However, for a while, we only discuss the averaged energies of these fragmented states to investigate the gross feature of the band structure and the fragmentation is discussed later. The averaged energy is calculated by multiplying w_i^J of the ith fragmented states as the weight; $E_{\rm AV}^J=\Sigma_i\, w_i^J E_i^J/\Sigma_i\, w_i^J$. When we compare the result of the deformed-basis AMD+GCM (solid lines in Fig. 2) and that of the $^{16}O+^{16}O$ GCM calculation (dashed lines in Fig. 2), $N=24$ band members obtained by the deformed-basis AMD+GCM are more deeply bound by about 10 MeV and their excitation energies are consistent with those obtained by the HF and HFB calculations and by the unique optical potential. The amount of the $^{16}O+^{16}O$ component of these band member states are around 50% which indicate the considerable distortion of the $^{16}O+^{16}O$ nature of this band. Therefore, we can conclude that the superdeformed band and the lowest $^{16}O+^{16}O$ molecular band ($N=24$) are identical bands which have a mixed structure of the deformed mean-field and the $^{16}O+^{16}O$ structure. The characteristics of $N=26$ and $N=28$ bands are different from that of the $N=24$ band. The excitation energies of these two bands obtained by the deformed-basis AMD+GCM are not so different from those obtained by the $^{16}O+^{16}O$ GCM as the case of the $N=24$ band. These small differences mean the enhancement of the $^{16}O+^{16}O$ molecular structure in the $N=26$ and $N=28$ bands. Indeed, the sum of the w^J of the fragmented states of these bands is much larger than that of the $N=24$ band member states; they amount to 0.71 and 0.73 in the case of 0^+ states of the $N=26$ and 28 bands, respectively.

Next, we try to improve our wave function to describe the enhancement of the $^{16}O+^{16}O$ structure in the excited bands. Since the variational calculation optimizes mainly the lowest $N=24$ band member states in which the $^{16}O+^{16}O$ molecular structure is distorted, basis states of the deformed-base AMD+GCM calculation can be inappropriate to describe the $N=26$ and $N=28$ bands in which the $^{16}O+^{16}O$ molecular structure is drastically enhanced. Therefore we have included the $^{16}O+^{16}O$ Brink wave functions in the basis states of the GCM calculation in addition to the deformed-basis AMD wave functions obtained from the variational calculation. The obtained results of the enlarged GCM calculation [deformed-basis+($^{16}O+^{16}O$)+GCM] are presented in Fig. 3. It is reasonable that the excitation energies of the $N=24$ band member states do not change, since in this band the molecular structure is distorted and the inclusion of the pure $^{16}O+^{16}O$ configuration is less important. On the contrary, in the $N=26$ and 28 bands the excitation energies are lowered by about a few MeV and the amount of the $^{16}O+^{16}O$ component has increased drastically. The sums of the fragmented w^J for the $N=26$ and 28 bands are 0.90 and 0.98, respectively.

Finally, we discuss the fragmentation of the $N=26$ and 28 band members. As an example, the energies and the amounts of the $^{16}O+^{16}O$ component for 0^+ fragments are listed in Table II. The 0^+ states of the $N=26$ and 28 bands are fragmented into three states. In the present calculation, the number of the fragments does not strongly depend on the angular

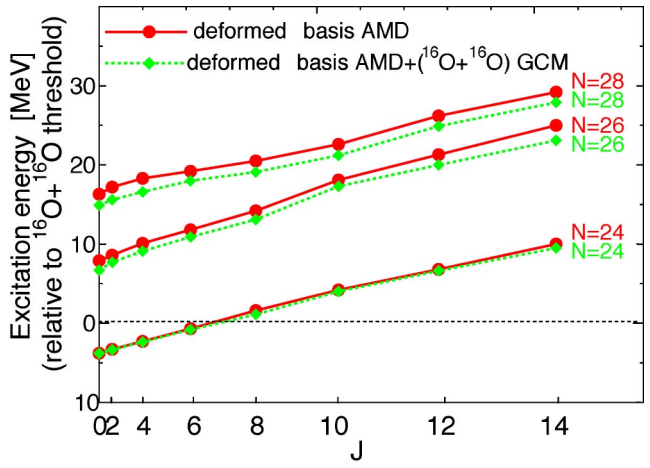

FIG. 3. (Color online) The excitation energies of the $N=24$, 26, and 28 band members obtained by the deformed-basis AMD+GCM (solid lines) and the deformed-basis AMD+($^{16}O+^{16}O$)+GCM (dotted lines). The $N=26$ and $N=28$ band members are fragmented into several states in both calculations and the averaged energies $E_{\rm AV}$ are shown for these bands. The deformed-basis AMD+GCM results in this figure are the same as those of Fig. 2.

momentum and the principal quantum number N. At most, the 10^+ state of $N=28$ band is fragmented into four states, while 11 fragments are observed. The fragmentations in our calculation are mainly caused by the coupling with the states with medium deformation which appear as a small peak between normal deformed states and the superdeformed states and also by the coupling with the $^{16}O+^{16}O^*$ states which are included in the very deformed ($\beta>0.9$) wave functions where $^{16}O^*$ stands for distorted $^{16}O^*$ cluster. Our model space is not large enough to be compared with the observed fragmentation. However, the fact that the fragmentation is obtained by the usage of the deformed-Gaussian basis is interesting. Details of these couplings are important to compare the present results and the experiments and will be investigated in our further study.

To summarize, we have shown that the superdeformed band obtained from the HF and HFB calculations and the Pauli-allowed lowest $N=24$ band of the $^{16}O+^{16}O$ molecular bands are essentially identical. In this band, $^{16}O+^{16}O$ molecular structure is distorted by the formation of the deformed mean-field and the spin-orbit force. This distortion is not small and lowers the excitation energy significantly, but these band members still have the considerable component

TABLE II. The excitation energies E_x and the amount w^J of the $^{16}O+^{16}O$ components of the fragmented 0^+ states of the $N=26$ and 28 bands.

	$N=26$		$N=28$	
	E_x	w^J	E_x	w^J
Fragment I	23.8	0.54	31.2	0.32
Fragment II	24.0	0.13	34.0	0.45
Fragment III	25.3	0.23	38.7	0.20
$E_{\rm AV}$ and Σw^J	24.2	0.90	33.7	0.98

of the $^{16}O+^{16}O$ molecular structure. We have obtained two excited bands which are generated by the excitation of the relative motion between two O clusters contained in the $^{16}O+^{16}O$ component of the superdeformed band. In the excited $N=26$ and 28 bands, the distortion is less important and the band members have the prominent molecular structure. The members of these bands are fragmented into several states.

The authors would like to thank Dr. Y. Kanada-En'yo for useful discussions. Most of the computational calculations were carried out by SX-5 at Research Center for Nuclear Physics, Osaka University (RCNP). This work was partially performed in the Research Project for Study of Unstable Nuclei from Nuclear Cluster Aspects sponsored by the Institute of Physical and Chemical Research (RIKEN).

[1] H. Friedrich, Nucl. Phys. **A224**, 537 (1974).
[2] D. Baye *et al.*, Nucl. Phys. **A258**, 157 (1976); **A276**, 354 (1977).
[3] T. Ando, A. Tohsaki, and K. Ikeda, Prog. Theor. Phys. **61**, 101 (1979); **64**, 1608 (1980).
[4] Y. Kondō, B. A. Robson, and R. Smith, in *Proceedings of the Fifth International Conference on Cluster Aspects in Nuclear and Subnuclear Systems, Kyoto, Japan*, edited by K. Ikeda *et al.* (Physical Society of Japan, Kyoto, 1988), p. 597; Phys. Lett. B **227**, 310 (1989).
[5] S. Ohkubo and K. Yamashita, Phys. Rev. C **66**, 021301(R) (2002).
[6] M. P. Nicoli *et al.*, Phys. Rev. C **60**, 064608 (1999); W. von Oertzen, H. G. Bohlen, and D. T. Khoa, Nucl. Phys. **A722**, 702 (2003).
[7] E. Stiliaris *et al.*, Phys. Lett. B **223**, 291 (1989).
[8] M. Yamagami and K. Matsuyanagi, Nucl. Phys. **A672**, 123 (2000).
[9] H. Molique, J. Dobaczewski, and J. Dudek, Phys. Rev. C **61**, 044304 (2000).
[10] R. R. Rodríguez-Guzmán, J. L. Egido, and L. M. Robledo, Phys. Rev. C **62**, 054308 (2000).
[11] T. Tanaka, R. G. Nazmitdinov, and K. Iwasaka, Phys. Rev. C **63**, 034309 (2001).
[12] T. Inakura *et al.*, Nucl. Phys. **A710**, 261 (2003).
[13] M. Bender, H. Flocard, and P.-H. Heenen, Phys. Rev. C **68**, 044321 (2003).
[14] M. Kimura, Phys. Rev. C **69**, 052404 (2004).
[15] J. A. Wheeler and J. J. Griffin, Phys. Rev. **108**, 311 (1957).
[16] J. Dechargé and D. Gogny, Phys. Rev. C **21**, 1568 (1980).
[17] Y. Kanada-En'yo and H. Horiuchi, Phys. Rev. C **52**, 647 (1995).
[18] Y. Kanada-En'yo and H. Horiuchi, Phys. Rev. C **68**, 014319 (2003).
[19] D. M. Brink, in *Many-Body Description of Nuclear Structure and Reactions*, Proceedings of the International School of Physics Enrico Fermi, Course 36, edited by Claude Bloch (Academic, New York, 1966).